

Supplementary Information

A DFT+U revisit on reconstructed $\text{CeO}_2(100)$ surfaces: structures, thermostabilities and reactivities

Chong-Yuan Zhou, Dong Wang and Xue-Qing Gong*

Key Laboratory for Advanced Materials, Centre for Computational Chemistry and Research Institute of Industrial Catalysis, School of Chemistry & Molecular Engineering, East China University of Science and Technology, 130 Meilong Road, Shanghai 200237, P.R. China

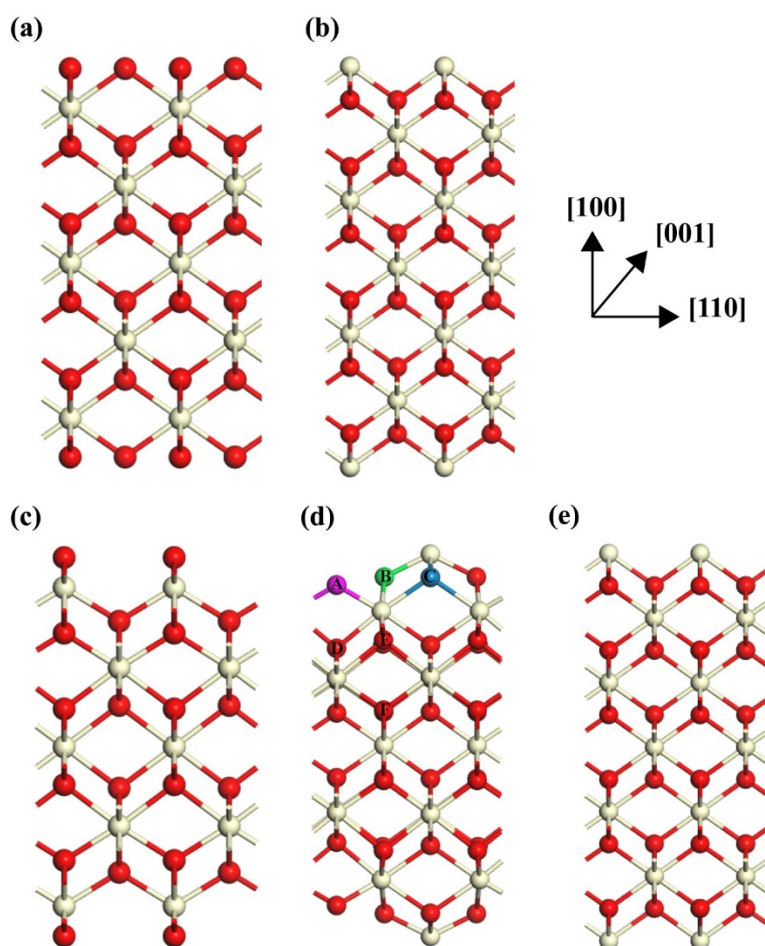


Figure S1 Structures of the intact (a, b) and reconstructed (c-e) $\text{CeO}_2(100)$ surfaces from the side views. (a) Intact $\text{CeO}_2(100)$ with a full layer of surface O; (b) intact $\text{CeO}_2(100)$ with a full layer of surface Ce; (c) reconstructed O-t surface with a half-layer of surface O; (d) reconstructed CeO_4 -t surface modeled by introducing CeO_2 units onto the O-t surface; (e) reconstructed Ce-t surface with a half-layer of surface Ce.

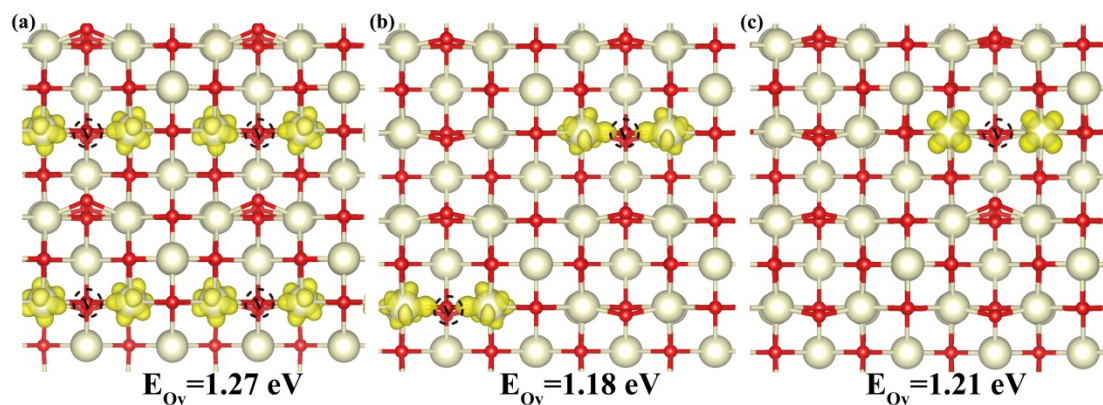


Figure S2 Calculated spin charge plots and average E_{O_v} values (per O_v) of O_v at the O^A site on the CeO_{4-t} surface using a $p(4 \times 4)$ model at the O_v concentration of (a) 100%, (b) 50%, and (c) 25%, respectively.

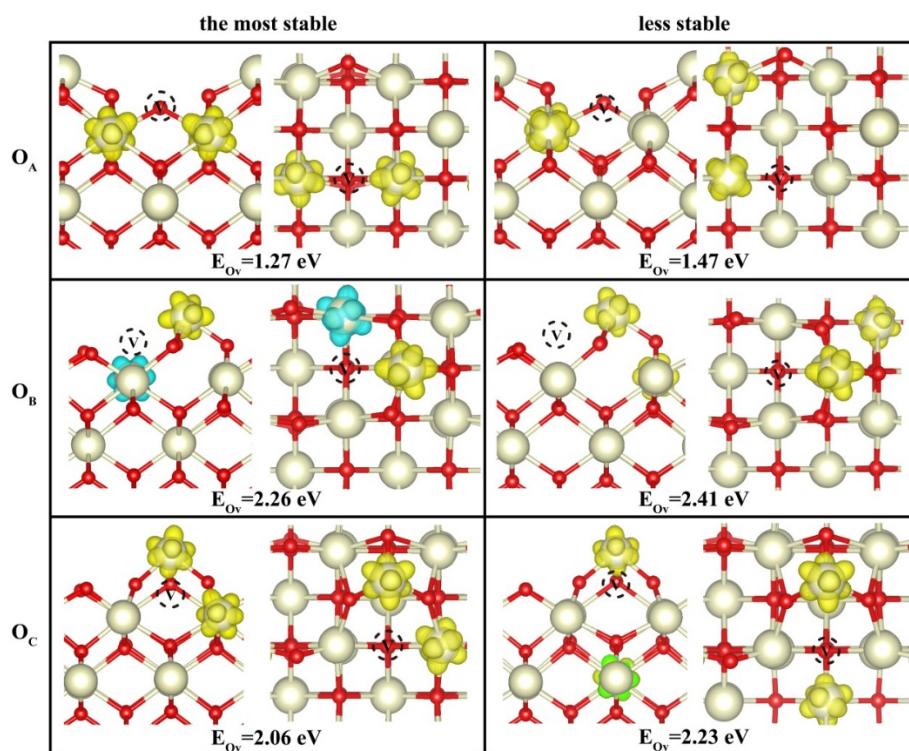


Figure S3 Calculated spin charge plots (side and top views) of the reduced CeO_{4-t} surfaces with the O_v at the (top row) O^A , (middle) O^B and (bottom) O^C sites, respectively, with both the most and less stable electronic configurations for the distributions of the localized electrons.

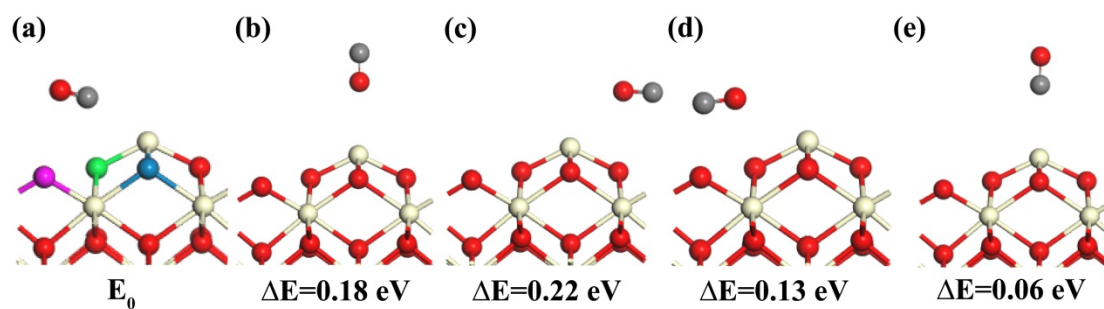


Figure S4 Calculated structures and relative energies of CO adsorption on the CeO_{4-t} surface. The calculated adsorption energy for CO at O^B (a) is 0.28 eV and it is taken as the reference.

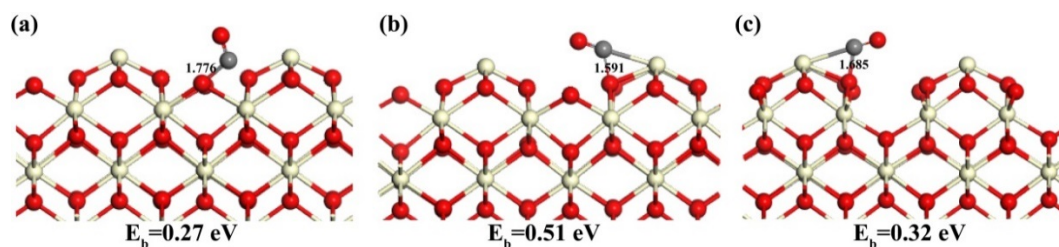


Figure S5 Calculated structures of transition states of CO oxidation via the channel of the (a) O^A, (b) O^B and (c) O^C on the CeO_{4-t} surface using a $p(4 \times 4)$ model. The corresponding reaction barriers are also listed.

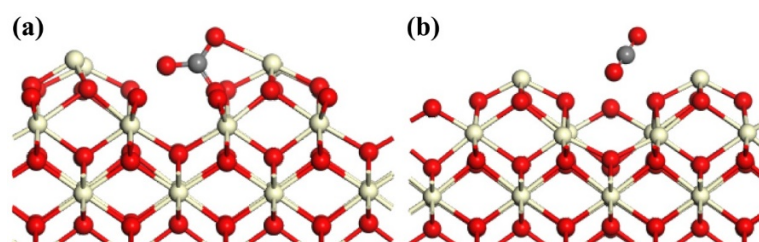


Figure S6 Calculated structures of the (a) carbonates species formed via the O^C channel and (b) the linear CO₂ via the O^A channel using a $p(4 \times 4)$ model.

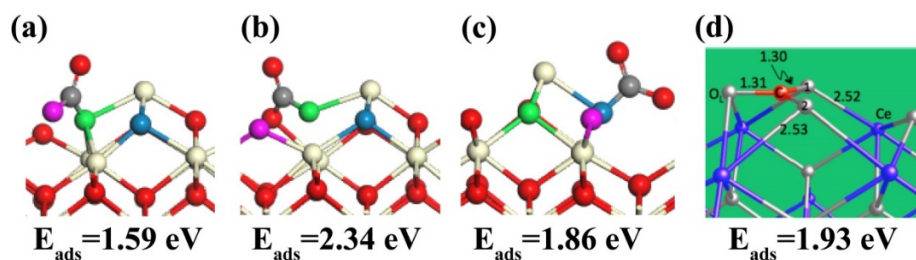


Figure S7 Calculated formation energies and structures of the carbonate species on (a-c) the $\text{CeO}_4\text{-t}$ type of reconstructed $\text{CeO}_2(100)$ from our work and (d) on the $\text{CeO}_2(100)$ surface reported by Mullins and co-workers. (ref. 39 in the main text).

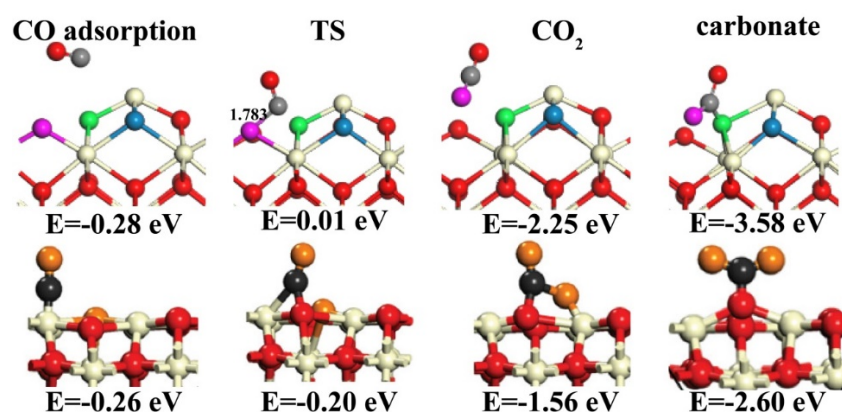


Figure S8 Calculated structures and energetics of CO oxidation from our results on the $\text{CeO}_4\text{-t}$ surface (top row) and the corresponding reverse processes of CO_2 reduction on the defective $\text{CeO}_2(110)$ reported by Lo and co-workers (bottom row; ref. 40 in the main text).